Domain-Inverted Electro-Optic Polymeric Waveguide Beam Deflector

Jeffery J. Maki[c], Guohua Cao[b], John M. Taboada[b], Huajun Tang[b], Suning Tang[a], and Ray T. Chen[b]

[a]Radiant Research, Inc., 9430 Research Blvd., Suite IV305, Austin, TX 78759-6543
[b]Microelectronics Research Center, Department of Electrical and Computing Engineering, The University of Texas at Austin, Austin, TX 78758-4445

ABSTRACT

A beam deflector has been designed and fabricated that uses a nonlinear-optical polymer. The device is composed of a cascade of polymeric electro-optic prisms formed within a planar waveguide of the same polymer system. A laser beam, to be deflected, is coupled into and out of the planar waveguide by cylindrical lenses. The light path of the laser beam within the planar waveguide is adjusted to pass through the successive prisms of the cascade, where the Gaussian transverse-mode profile is centered (initially) within each of the prisms. The index of refraction of each prism in the cascade, but not of the surrounding polymer, is modified by the electro-optic effect when a drive voltage is then applied. The application of a drive voltage thus causes the planar waveguide to function as a sequence of prisms that change the path of propagation of the beam through the planar waveguide. The collimated beam formed by the output cylindrical lens deflects. The extent of deflection is proportional to the amount of refractive-index change induced in the prism cascade. A uniform electrode structure can drive the electro-optic prism cascade, which should enable the device to operate at high speeds when traveling-wave driven.

Keywords: deflector, scanner, steerer, laser beam, prism, planar waveguide, polymer, second-order nonlinear optics, electro-optic effect, traveling-wave electrode

1. INTRODUCTION

Many schemes for deflecting, steering, or scanning a laser beam have been investigated since the invention of the laser, which are motivated by the many laser applications that require the propagation direction of the beam be redirected. The many different schemes each have a different set of applications and operating limitations. Current beam deflectors have limitations that include large drive voltage, low speed of operation, small angle of deflection, and bulky size. Beam deflectors that alleviate these performance limitations are of interest because they may make possible new applications and would enhance the performance of such current devices as optical memories, printers, page scanners, optical switches, and displays.

One class of schemes for deflecting a laser beam makes use of the electro-optic effect, which occurs in materials possessing a second-order nonlinear-optical response. Bulk inorganic crystals, such as $LiNbO_3$ and KD*P, have been used to construct beam deflectors. The crystals are cut in the shape of one or more prisms and the electro-optic effect is used to adjust the refractive index of each prism, which varies the amount of deflection.[1-3] These bulk, electro-optic, prism deflectors have the advantage of large clear apertures, but require voltages on the order of thousands of volts to drive them. In another related scheme, electro-optic crystals are used to make "digital" beam deflectors,[4,5] which deflect a laser beam to discrete output paths only. The need for deflectors in integrated-optic applications has lead to the use of waveguide geometries. Planar electro-optic waveguides are formed on the surface of bulk crystals.[6-8] The electric field to drive the electro-optic effect is applied through a set of electrodes placed only on top of the planar waveguides. These electrodes induce a spatially-defined refractive-index profile across the planar waveguide that emulates a prism and, hence, causes variable beam deflection within the plane of the planar waveguide. The drive voltage continues, though, to be fairly large because of the large overall spacing of the top electrodes. There is, furthermore, a problem of electrical breakdown (shorting) in these electrode structures. A

Further author information—
J.J.M. (correspondence): Email: RRIjjmPhD@aol.com, WWW: http://members.aol.com/RRIsales/, Telephone: 512-338-4521, Fax: 512-338-4645

relatively recent approach has been to use wafers of electro-optic crystal with electrodes placed on opposite sides of the wafer.[9,10] The required drive voltage is thus lowered substantially owing to the use of an electro-optic crystal that has been thinned to a few hundred microns. The electrodes are uniform in this approach. The electro-optic prism response is created by inverting the domains of the electro-optic crystal in prism-shaped regions. The electric-field induced change in the refractive index is opposite in sign in these domain-inverted regions compared to the surrounding material. This scheme not only provides for reduced drive voltages, but the need for only uniform electrodes also allows for the use of a traveling-wave drive source for higher speeds of operation.

Beam deflectors constructed from electro-optic polymer[11] promise to match or exceed the performance characteristics of electro-optic-crystal deflectors in the areas of deflection angle, drive voltage, and speed of operation. The key enabling factor is that electro-optic polymer can be spin coated into thin films that are only a few microns in thickness. Electrodes can be easily formed on opposite sides of the cladding layers of the waveguide during fabrication. The required drive voltage is reduced dramatically over that required by the much thicker wafer electro-optic-crystal deflectors. Instead of inverting domains in an electro-optic crystal to from prisms, prism regions in a polymer planar waveguide can be produced by poling the polymer in only those regions. After fabrication and poling, the electro-optic effect will occur only in the prism regions when a drive voltage is applied by a uniform electrode. The efficiency with which the applied voltage can produce an electric field within the polymer films allows for a reduced voltage with polymer-based deflectors to achieve the same change in the refractive index as in inorganic-crystal deflectors. Thus, for equal voltages, the induced change in the refractive index is larger in polymer deflectors and, hence, the deflection can be larger. The low value of the dielectric constant for polymer over that for inorganic crystals enables the possibility of even higher speeds of operation.

In this paper, we report the first demonstration of a compact laser-beam deflector based on electro-optic prisms formed within a thin-film polymer waveguide. We first review the details of the device concept in Sec. 2. The anticipated deflection angle is calculated for a nonlinear-optical-polymer-based beam deflector. In Sec. 3, we describe some of the devices we have constructed to investigate the use of electro-optic polymer to make beam deflectors. We overview the various fabrication techniques used. Beam deflection is demonstrated in Sec. 4 using our polymer-waveguide devices. In Sec. 5, we give some conclusions about our research into polymeric beam deflectors.

2. DEVICE CONCEPT

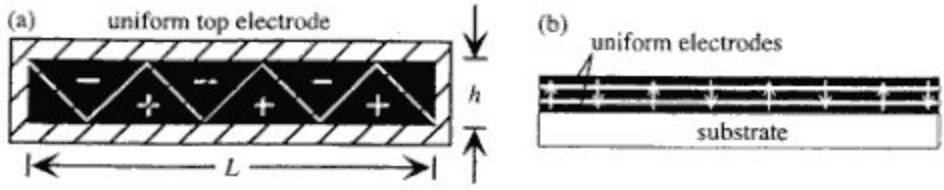

FIG. 1. Schematic of the device concept for achieving beam deflection using an electro-optic polymer. (a) Top view showing the prism-shaped regions driven by a uniform electrode. The "+" and "−" signs indicate the sign of the electro-optic coefficient in each region; the domain orientation. (b) Side view showing the alternating sign of the electro-optic response (as depicted by the arrows) even though the electric-field lines are in the same direction for each domain.

The essential elements of a planar-waveguide beam deflector based on electro-optic polymer is shown in Fig. 1. The prism shaped regions are created by poling the polymer in only those regions. By reversing the sign of the poling voltage, some of the regions can be made to have an electro-optic coefficient that is opposite in sign. We have marked these two regions "+" and "−". When a positive voltage is applied to the uniform electrode, the index of refraction will decrease in the "+" regions by Δn_+ and it will increase in the "−" regions by Δn_-. For a negative applied voltage, opposite signs of refractive-index change will occur. The use of the interleaved prism regions of opposite electro-optic response allows for the most effective use of the electro-optic effect in polymer, since the total index change is $\Delta n_+ + \Delta n_- = 2\Delta n$, which is twice that occurring in either type of domain. Both types of regions need not possess the electro-optic effect in order to produce beam

deflection. One of the regions, say the "–" regions, could be composed of polymer that is not poled; and, hence, does not respond to the applied voltage. The overall refractive index change would then be half as large.

The laser beam to be deflected travels from one end of the planar-waveguide device to the other. When the beam deflector is activated by an applied voltage, the laser beam deflects off of the initial optical axis, where the sign of deflection depends upon the sign of the induced overall change in the refractive index. The amount of deflection is controlled by the amount of index difference induced in the polymer by the electro-optic effect. For a given index difference, refraction at each successive prism interface adds up to cause a net deflection of the beam. In related research, multiple prisms are placed transverse to the propagation direction. This configuration has come to be known as an array of prisms, while prisms along the propagation direction are known as a cascade.[3] The amount of electro-optic-induced beam deflection (in radians) of a cascade-type deflector of interleaved, domain-inverted, prisms of equal height/width h is[12]

$$\Delta\theta = 2\Delta n \frac{L}{h} , \tag{1}$$

where L is the length of the prism cascade. The number of prisms does not enter into the formula directly. The formula would remain the same for one or many prism interfaces making up the deflector.

The beam deflector envisioned here has prism regions poled in a direction that is perpendicular to the plane of the planar waveguide. Thus, for TM polarized light in the waveguide, which is also an extraordinary ray, the electro-optic effect induces a refractive index difference

$$\Delta n(V) = n_e(0) - n_e(V) = \frac{1}{2} n_e^3 r_{33} \frac{V}{d_{\text{eff}}} , \tag{2}$$

where $n_e = n_e(0)$ is the extraordinary refractive index at zero applied voltage and r_{33} is the appropriate electro-optic tensor component, which is assumed to be positive and negative for the "+" and "–" domains, respectively. The voltage applied across the electrodes is V and d_{eff} is the effective distance across which the voltage would be dropped to yield the actual electric-field strength that drives the EO response. The effective thickness d_{eff} can be modified by changing the actual physical separation d of the top and bottom electrodes, which is determined by the thickness of the waveguide core and cladding layers. This effective distance is computed using

$$d_{\text{eff}} = d_w + \frac{\varepsilon_w}{\varepsilon_c} d_c , \tag{3}$$

where d_w, d_c, ε_w, and ε_c are the thicknesses and permittivities of the waveguide core and cladding, respectively. The typical values of d_{eff} are between 6 and 10 μm. The thickness d is set by issues of the optical throughput of the waveguide core, optical loss owing to interaction of the waveguide evanescent optical fields with the electrodes through the cladding layers, and details of the poling step. For a given electro-optic polymer system, these thicknesses are typically optimized and then held fixed. Therefore, the geometrical size parameters readily available for adjustment are only the shapes of the prisms, which here amounts to choosing the values of L and h.

The nonlinear-optical material response determining the amount of deflection is completely contained in the factor $n_e^3 r_{33} / d_{\text{eff}}$. The numerical value of this factor allows for direct comparison of the efficiency of deflection with voltage between various material systems used to construct a beam deflector of the type described here. For the electro-optic polymer system LD-3 that we are using,[14] we have achieved $r_{33} = 18$ pm/V at 632.8 nm,[15] which is a numerical value other polymer systems can reach or exceed.[16] This gives $n_e^3 r_{33} / d_{\text{eff}} = 7.7 \times 10^{-6}\ V^{-1}$, where we have used $n_3 = 1.62$ and $d_{\text{eff}} = 10\ \mu$m. The most recent demonstration of a $LiTaO_3$ beam deflector[13] has a wafer thickness giving $d_{\text{eff}} = 474\ \mu$m. Since $n_3 = 2.18$ and $r_{33} = 30.5$ pm/V at 632.8 nm for $LiTaO_3$, $n_e^3 r_{33} / d_{\text{eff}} = 6.6 \times 10^{-7}\ V^{-1}$, which is an order of magnitude lower in value than that for our polymer. Thus the performance of polymer tends to exceed the performance of inorganic crystal because of the small thickness readily achievable with spin-coated polymer.

The amount of beam deflection can be predicted using Eq. (1) with $n_e^3 r_{33} / d_{eff} = 7.7 \times 10^{-6} V^{-1}$. The remaining quantity to be specified that Eq. (1) requires is the ratio of L and h. The large surface area of planar waveguides made from spin-coated polymer allows for device geometries where $L/h = 100$. Equation (1) with these parameter values gives 1° of deflection for 23 V of applied voltage. The utility of this amount of beam deflection is best described by the total number of possible resolvable spots the beam can be deflected. The number of resolvable spots for a Gaussian beam, with its beam waist located at the center of the beam deflector, is

$$N = 2\frac{\Delta\theta}{\theta_{div}} + 1 , \tag{4}$$

where $\theta_{div} = \lambda / \pi w_o$ is the divergence angle of the Gaussian beam. In deriving Eq. (4), we have assumed the deflector will be used to deflect a beam in both the positive and negative directions. In order to deflect the entire laser beam, the beam waist should be contained within the height/width of the prism h. A consistent choice would be to set $w_o = h/2$, which gives the number of resolvable spots to be

$$N = 2\frac{\pi\Delta n}{\lambda} L + 1 , \tag{5}$$

Equation (5) is independent of the height/width h of the prisms. Of the geometrical factors L and h, it is only the length L of the prism cascade that determines the number of resolvable spots for an optimally illuminated deflector device.

3. FABRICATION

FIG. 2. Microscope photograph of the polished end face of an LD-3/NOA-61 planar waveguide. Not visible are the gold top and bottom electrodes.

We have fabricated planar waveguides using polymer. The waveguide core material is based on LD-3, which is a double-ended thermally-crosslinked polymer consisting of a poly-methyl-methacrylate (PMMA) backbone and an azobenzene-sulfone chromophore.[14] It can be readily poled and cured through the simultaneous application of a poling voltage and heat. The application of heat causes the small crosslinker molecules dianisidine diisocyanate that are added to the LD-3 polymer to form covalent bonds with the LD-3 polymer chain. The material, hence, becomes a fully crosslinked polymer matrix. When the poling electric field is removed and the device returns to a nominal temperature, the poling induced orientation of the NLO chromophores is essentially locked in place because of the complete crosslinking. The cladding material is Norland Optical Adhesive 61 (NOA-61), which is a UV-curable resin. The waveguides have been fabricated on silicon substrates by spin coating. The solvent used is cylopentanone rather than tetrahydrofuran as was used in the initial demonstrations of waveguides fabricated using LD-3.[17] Shown in Fig. 2 is a photograph of the polished end face of one of our planar waveguides. The thickness of the core material is 4.0 μm and the thickness of the two cladding layers are each 2.4 μm. The silicon substrate has a uniform coating of gold placed on it before the polymer layers are deposited. A second gold electrode is placed on top of the LD-3/NOA-61 polymer layers.

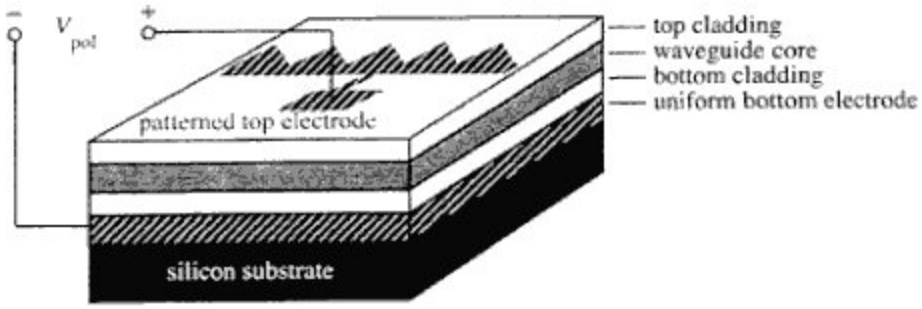

FIG. 3. Method of poling the polymer waveguide core using a patterned top electrode and a uniform bottom electrode, which creates domains within the polymer core that possess a second-order optical nonlinearity.

Figure 3 shows the arrangement used to pole the planar waveguide sample in prism shaped regions. An actual top gold poling electrode is shown in Fig. 4(a). The electrode is patterned by wet etching. The top electrode consists of five prism-shaped regions of thin-film gold. Each prism is connected at its base to the next prism. A contact pad has been placed to allow for easy application of the driving voltage. The poling arrangement shown in Fig. 3 produces a cascade of prisms all poled in the same direction rather than an interleaved set of domain-inverted prisms as described above. The amount of beam deflection a single-domain prism-cascade device can produce is 50% of a cascade of interleaved domain-inverted prisms. When a voltage is applied to the electrode structure shown in Fig. 3 to pole the polymer core, the electric field lines extend from the top electrode to the bottom electrode, which is uniform. Since the various polymer layers are very thin, the field lines do not extend out beyond the edge of the top electrode by any appreciable extent. The polymer is thus poled essentially in only the regions where the patterned top electrode exists. After the polymer is poled, the patterned poling electrode is replaced by a uniform drive electrode. Actually, for our test devices, more metal is deposited over the patterned poling electrode to form a uniform electrode [see Fig. 4(b)]. Aluminum is used in this case. The device shown in Fig. 4(b) is thus our concept-demonstrating device. The edges of the device at each end of the prism cascade are polished to allow light to be coupled into and then out of the polymer planar waveguide, so that a laser beam to be deflected can pass through without disruption of its Gaussian mode profile.

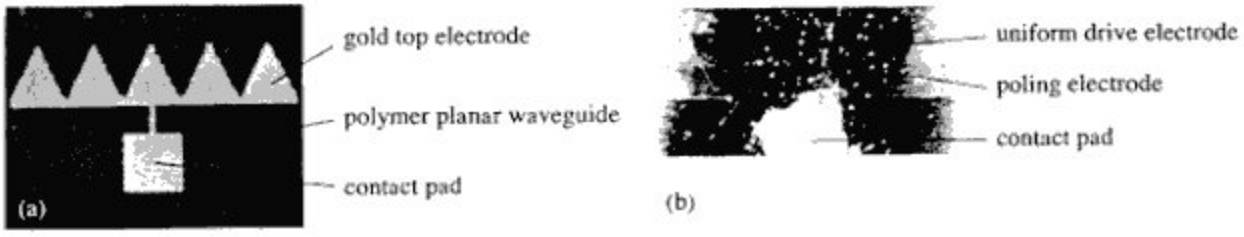

FIG. 4. Close-up photographs of a beam-deflector device during (a) fabrication, which shows the patterned gold electrode used to pole the device, and (b) after fabrication, which shows the uniform aluminum drive electrode coated over the patterned poling electrode.

We have developed a technique of poling polymer that uses a top electrode that is placed in electrical and physical contact with the polymer by a conducting liquid.[15] Hence, this form of poling is called liquid-contact poling. We are pursuing liquid-contact poling as a means of poling the prism regions, since it has proven to be a good method of poling polymer waveguides that have a high value of the electro-optic coefficient and are low in loss.[15] The idea is to pattern the liquid-contact electrode, so that the conducting liquid is only in contact with the polymer in prism-shaped regions. In pursuing the use of liquid-contact poling to pole prism shaped regions, we have first constructed beam deflectors that are poled uniformly by the liquid-contact method. Since the electric-field lines are well localized by a patterned top electrode, it should be possible to achieve beam deflection using a uniformly poled polymer waveguide with a patterned top electrode. Even though the entire polymer waveguide is poled and thus possesses an electro-optic response, the electro-optic effect occurs only where the

driving electric field is present. We have constructed such a device. After the sample is poled and cured, the liquid-contact electrode is removed and the surface of the polymer waveguide is cleaned. A patterned gold electrode is then produced on top of the polymer waveguide. This prism electrode structure on top of the poled polymer looks essentially like one of our patterned electrodes for metal-contact poling as shown in Fig. 4(a).

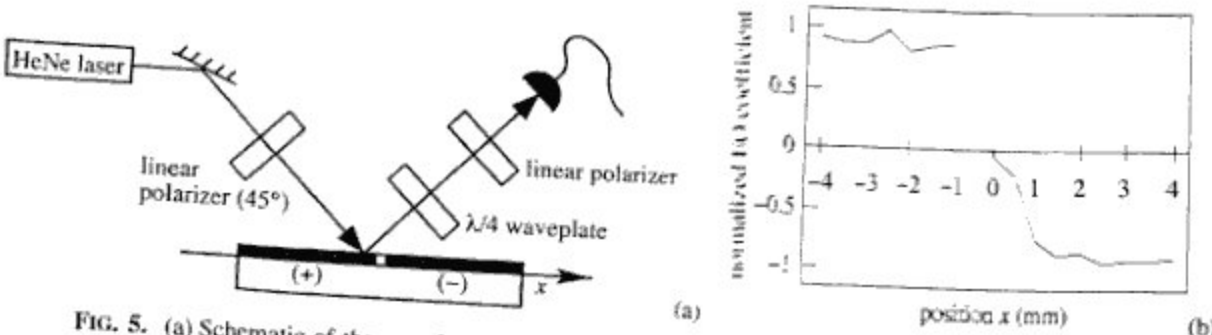

FIG. 5. (a) Schematic of the experimental setup using the reflection technique to measure the magnitude and relative sign of the electro-optic coefficient. (b) Recorded signal showing the change in sign of the electro-optic coefficient r_{33}.

We have investigated domain-inverted poling of LD-3 polymer, which is a technique necessary to make the interleaved cascade of prisms as shown in Fig. 1. Rectangular regions are poled by the simultaneous application of static poling voltages that are of equal magnitude but opposite polarity in the two regions. Liquid-contact poling is used. The bottom electrode is uniform over the area of the two regions to be poled. The top electrode is two rectangular regions of indium-tin-oxide (ITO) patterned on a glass plate with a gap of approximately 2 mm to isolate the two electrodes electrically. This top electrode structure is placed in contact with the polymer film using hexatriacontane, which melts at 75°C and becomes electrically conductive. The conductivity is larger than that of the polymer, but not so large as to cause a short across the gap. The top ITO-electrode structure is held at a spacing of approximately 10 μm from the surface of the polymer by epoxy spacers. A static poling voltage of 275 V is applied across each region at a temperature of 165°C for 55 minutes, which poles and cures the polymer. We demonstrate that the two regions are poled in opposite directions (i.e., domain inverted) by measuring the electro-optic coefficient of each region using an extension of the reflection technique of Teng and Man.[18] The experimental setup is shown in Fig. 5(a). The sample is driven by a voltage with the same magnitude and polarity for each of the two regions. The applied voltage is $V_m \sin(\omega_m t)$, which oscillates at the angular frequency ω_m, where the peak voltage is V_m. The HeNe laser beam at 632.8 nm impinges upon the sample with equal amounts of s and p polarization. The reflected light picks up a phase lag dependent upon the magnitude and sign of the electro-optic effect. After passing through the $\lambda/4$ waveplate and the linear polarizer, this phase lag turns into an intensity modulation whose magnitude depends upon the strength of the electro-optic effect. The total intensity received by the photodetector is

$$I(x) = I_o + I_m(x) , \tag{6}$$

where I_o is the unmodulated portion of the total intensity. The essential contributions to the modulated intensity are given by

$$I_m(x) \propto r_{33}(x) V_m \sin(\omega_m t) . \tag{7}$$

Equation (7) makes explicit the dependence of the modulated intensity upon the spatial variation of the poling-induced electro-optic coefficient r_{33}. We use a lock-in amplifier to measure the portion of the optical signal oscillating at angular frequency ω_m. For the signal coming from reflection off of the "+" region, the phase of the lock-in amplifier is set to make the signal positive and maximum in value for one of the quadratures. As the sample is translated over to the "−" region, the magnitude and sign of this quadrature signal is recorded. The result is shown in Fig. 5(b). The signal changes sign as the probing laser beam crosses over from one region to the other. There is some variation of the magnitude of the response in the gap region. Figure 5(b) shows that the two regions have electro-optic coefficients r_{33} that are opposite in sign.

4. PERFORMANCE CHARACTERIZATION

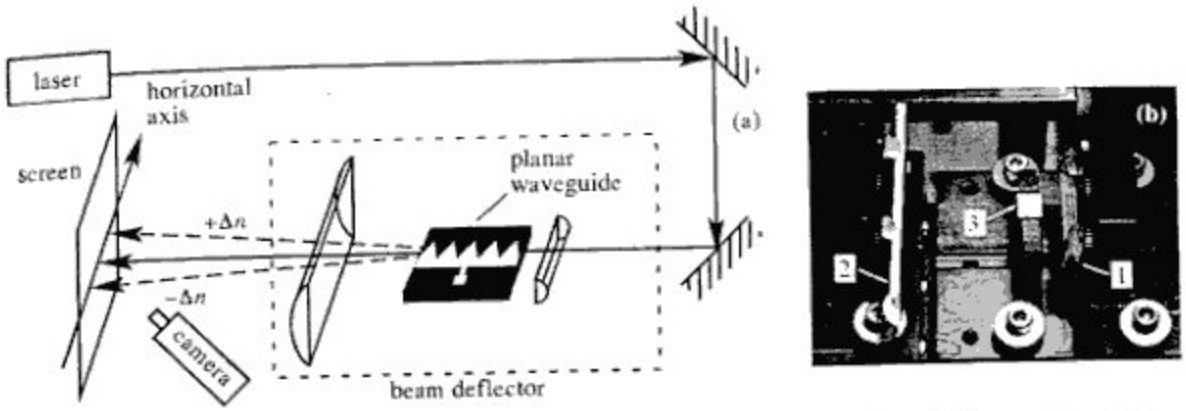

FIG. 6. (a) Schematic of the beam-deflector test bed and (b) photograph of the beam deflector. The screen for observing the beam deflection is placed 2 ft. (610 mm) from the center of the planar waveguide sample. Cylindrical lenses "1" (6.35 mm focal length) and "2" (25.4 mm focal length) couple the TM-polarized laser beam into and out of the planar waveguide "3," respectively. The electrical connections to apply the DC drive voltage are not shown.

Shown in Fig. 6(a) is the experimental setup to demonstrate the polymeric beam deflector shown in Fig. 6(b). The planar waveguide sample is mounted on a sample stage with two cylindrical lenses. The laser is a grating-feedback diode laser from New Focus, which has been set to operate at 790 nm. The laser has a good Gaussian intensity profile as shown in Fig. 7. The laser is coupled into the planar waveguide of the beam deflector using a somewhat short focal-length lens ($f = 6.35\,\text{mm}$). After propagating through the planar waveguide, the beam exits the waveguide and is recollimated by a longer focal-length lens ($f = 25.4\,\text{mm}$). As Fig. 6 depicts, an opaque white-board screen is placed 2 ft. (610 mm) away from the center of the prism cascade of the beam deflector. The transmitted laser beam is incident upon the screen. A video camera is placed to view the spot formed on the screen. The video camera output is recorded as still images by a frame grabber and stored as digital images for later analysis. The profile of the laser beam through its center can then be extracted and the intensity plotted versus position. These profiles can also be fitted to the Gaussian intensity-profile function

$$I = I_{\text{background}} + I_o \text{Exp}\left[-2(x - x_o)^2 / w^2\right] , \tag{8}$$

where x_o is the location of the peak intensity value and w is the spot-size radius. The curve fitting helps to more precisely locate the peak intensity (i.e., the center of the spot) and to characterize the beam shape.

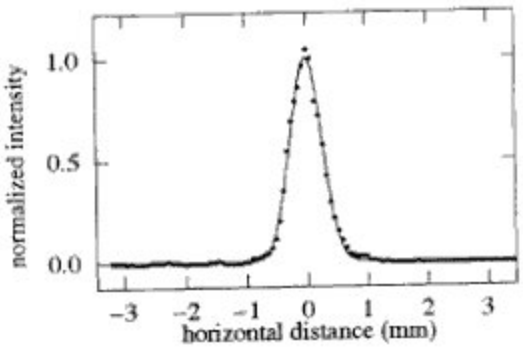

FIG. 7. Intensity profile of the laser beam measured 190 mm before reaching the beam deflector. The smooth line is the best fit to the data by a Gaussian curve.

The specific geometry of the prism design we are using is given in Fig. 8. The design has five equal-sized prisms of height $h = 1$ mm, which form a cascade of length $L = 5$ mm. The device thus has a ratio $L/h = 5$. The performance can be improved by decreasing the height h to 0.5 mm and increasing the length L to 5 cm. The combined affect would be to raise the ratio to $L/h = 100$, which is a factor of 20× increase in L/h over the value for the current design. Of course, there are many choices for the value of L and h that increase the value of L/h. Clearly, though, the height h of the prisms, which is the width of the active-region of the device, should be as small as possible to increase the deflection sensitivity with voltage, but large enough to contain the laser beam profile.

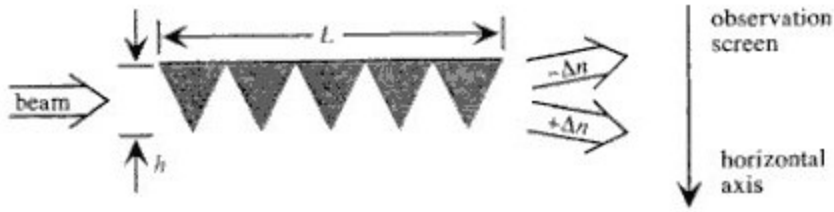

FIG. 8. Schematic of the prism-cascade concept device for demonstrating beam deflection using an electro-optic polymer. The prism cascade is 5 mm in total length L, where each prism is 1 mm in height h.

We have observed beam deflection using our electro-optic-polymer prism-cascade devices. The experimental setup given in Fig. 6 is used to record the beam deflection. The beam deflects in the negative horizontal direction (as defined in Fig. 8) for negative values of the induced index difference Δn and in the positive horizontal direction for positive values of the induced index difference Δn. Figure 9 shows pictures of the recorded laser-beam spots. The electro-optic induced index difference is $+\Delta n$ for positive deflection and $-\Delta n$ for negative deflection, where $\Delta n = 2.5 \times 10^{-4}$. Note that the horizontal axis is calibrated by taking a picture of a ruler marked in millimeters, which is placed on the screen at the location of the incident laser beam. From this calibration, we calculate that the range of deflection is 0.14° for $\Delta n = 2.5 \times 10^{-4}$. The number of resolvable spots is not optimal. We have under illuminated the prism cascade. We could have used a laser beam that was recollimated with a larger Gaussian-beam waist located at the beam deflector, which would have reduced the amount of beam divergence and thus increased the number of resolvable spots.

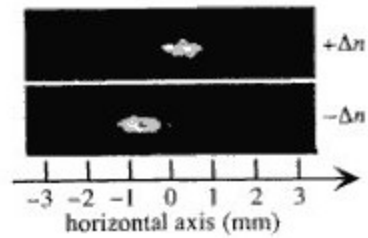

FIG. 9. Images of the transmitted laser beam incident upon the observation screen for positive and negative values of induced index difference, where $\Delta n = 2.5 \times 10^{-4}$.

Figure 9 also shows that all of the beam is deflected. There is no residual undeflected beam. The process of refraction of the laser beam as it passes through each of the successive prisms of the cascade has redirected the path of the laser beam entirely. This is very different from beam deflectors that use diffraction,[8] where a portion of the beam is not deflected because the diffraction efficiency is typically not 100%.

We have extracted the intensity profiles of the spots recorded on the screen and have fitted them using the Gaussian-profile function given in Eq. (8). Figure 10 shows the results for three example profiles. The beam profiles of the transmitted laser beam fit a Gaussian profile quite well. The average spots-size radius of the beams measured at the screen is $w = 0.9$mm.

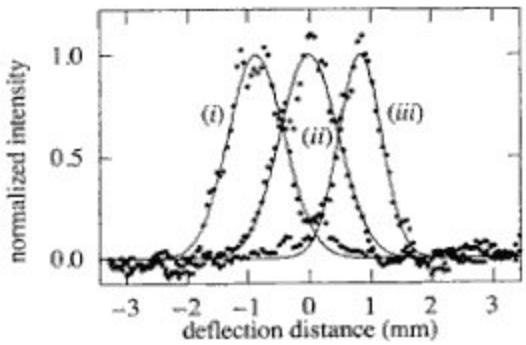

FIG. 10. Intensity profiles of the transmitted laser beam incident upon the observation screen for (*i*) negative horizontal deflection ($\Delta n = -2.5\times 10^{-4}$), (*ii*) no deflection ($\Delta n = 0$), and (*iii*) positive horizontal deflection $\Delta n = +2.5\times 10^{-4}$. The smooth curves are fits of the measured profiles to the Gaussian intensity-profile function given by Eq. (8).

The amount of beam deflection is quantified in Fig. 11 as a function of the electro-optic-induced index difference Δn. The location of the beam along the horizontal axis is taken to be the location of the peak-intensity value, which is the best-fit value of x_o. For $\Delta n = 0$, the value of x_o determines the origin. For increasing values of the magnitude of Δn, the beam deflects more and hence x_o increases in magnitude, where the sign of the deflection depends on the sign of Δn. A straight line has been fitted to the data points in Fig. 11.

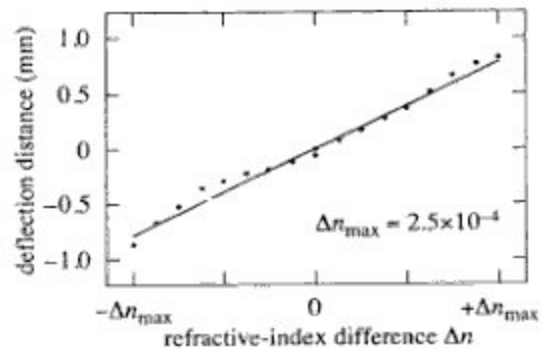

FIG. 11. Electro-optic-induced deflection of the transmitted laser beam quantified by measuring the displacement x_o on the observation screen of the peak intensity from its location for zero index difference Δn.

5. CONCLUSIONS

We have demonstrated beam deflection using a cascade of prisms whose index of refraction is varied using the electro-optic effect. The deflection efficiency is observed to be nearly 100%; there is some weak scattered light. In addition, the laser beam maintains its Gaussian intensity profile after propagating through the device. The initial device design is not optimal. It was constructed to prove the beam-steering concept in a straight-forward manner. To increase the number of resolvable spots, the device should be made longer as is indicated by Eq. (5). The device can also be improved upon by departing from the use of a cascade of equal-sized prisms. Not discussed in the context of Eq. (5) is the fact that, as the beam propagates through the device, it deflects farther from the initial optical axis. Thus the prisms near the output end need to be larger to continue to encompass the entire beam profile. A more optimal design would have a cascade of prisms of increasing size from the input end towards the output end. Nonetheless, the performance of this initial device has generated much excitement in pursuing this approach as a means of redirecting a laser beam. Since this device adds to the other devices that can be constructed in thin-film polymer, it opens up the possibility of new integrated-optic devices made in combination.

6. ACKNOWLEDGEMENTS

This research program was supported by the Office of Secretary of Defense (OSD) and 3M.

7. REFERENCES

1. T. C. Lee and J. D. Zook, "Light beam deflection with electrooptic prisms," *IEEE J. Quantum Electron.*, vol. QE-4, no. 7, pp. 442–454, 1968.
2. J. F. Lotspeich, "Electrooptic light-beam deflection," *IEEE Spectrum*, vol. 5, pp. 45–53, Feb. 1968.
3. Y. Ninomiya, "Ultrahigh resolving electrooptic prism array light deflectors," *IEEE J. Quantum Electron.*, vol. QE-9, no. 8, pp. 791–795, 1973.
4. R. K. Lee, Jr. and F. Moskowitz, "Transmission and self-generated noise characteristics of polarization scanned digital optical systems," *Appl. Opt.*, vol. 3, no. 11, pp. 1305–1310, 1963.
5. G. Hepner, "Digital light deflector with prisms and polarization switch based on the Pockels effect with transverse field," *IEEE J. Quantum Electron.*, vol. QE-8, no. 2, pp. 169–173, 1972.
6. P. K. Tien, S. Riva-Sanseverino, and A. A. Ballman, "Light beam scanning and deflection in epitaxial $LiNbO_3$ electro-optic waveguides," *Appl. Phys. Lett.*, vol. 25, no. 10, pp. 563–565, 1974.
7. C. S. Tsai and P. Saunier, "Ultrafast guided-light beam deflection/switching and modulation using simulated electro-optic prism structures in $LiNbO_3$ waveguides," *Appl. Phys. Lett.*, vol. 27, no. 4, pp. 248–250, 1975.
8. C. H. Bulmer, "Electro-optic waveguide deflectors," *Proc. SPIE*, vol. 176, pp. 4–11, 1979.
9. Q. Chen, Y. Chiu, D. N. Lambeth, T. E. Schlesinger, and D. D. Stancil, "Guided-wave electro-optic beam deflector using domain reversal in $LiTaO_3$," *J. Lightwave Tech.*, vol. 12, no. 8, pp. 1401–1404, 1994.
10. M. Yamada, M. Saitoh, and H. Ooki, "Electric-field induced cylindrical lens, switching and deflection devices composed of the inverted domains in $LiNbO_3$ cyrstals," *Appl. Phys. Lett.*, vol. 69, no. 24, pp. 3659–3661, 1996.
11. *Nonlinear optics of organic molecules and polymers*, ed. by H. S. Nalwa and S. Miyata, CRC Press, New York, 1997.
12. A. Yariv, *Quantum Electronics*, Sec. 14.7, John Wiley & Sons, New York, 1975.
13. V. Gopalan, M. J. Kawas, M. C. Gupta, T. E. Schlesinger, and D. D. Stancil, "Integrated quasi-phase-matched second-harmonic generator and electrooptic scanner on $LiTaO_3$ single crystals," *IEEE Photonics Tech. Lett.*, vol. 8, no. 12, pp. 1704–1706, 1996.
14. C. Xu, B. Wu, O. Todorova, L. Dalton, Y. Shi, P. M. Ranon, and W. H. Steier, "Stabilization of the dipole alignment of poled nonlinear optical polymers by ultrastructure synthesis," *Macromolecules*, vol. 26, no. 20, pp. 5303–5309, 1993. (LD-3 is Polymer 2 in this paper.)
15. H. Tang, J. M. Taboada, G. Chao, R. L. Li, and R. T. Chen, "Enhanced electro-optic coefficient of nonlinear-optical polymer using liquid-contact poling," *Appl. Phys. Lett.*, vol. 70, no. 5, pp. 538–540, 1997.
16. A. W. Harper, S. Sun, L. R. Dalton, S. M. Garner, A. Chen, S. Kalluri, W. H. Steier, and B. H. Robinson, "Translating microscopic optical nonlinearity to macroscopic optical nonlinearity: The role of chromophore-chromophore electrostatic interactions," *J. Opt. Soc. Am. B*, in press.
17. P. M. Ranon, *Second-order optical properties study and the poling induced dipole alignment stabilization of second-order nonlinear optical polymers*, Ph.D. dissertation, Univ. S. Calif., 1993.
18. C. C. Teng and H. T. Man, "Simple reflection technique for measuring the electro-optic coefficient of poled polymers," *Appl. Phys. Lett.*, vol. 56, no. 18, 1734–1736, 1990.